



Room Temperature Characterization of a Magnetic Bearing for Turbomachinery

Gerald Montague

U.S. Army Research Laboratory, Glenn Research Center, Cleveland, Ohio

Mark Jansen

Sest, Inc., Brook Park, Ohio

Andrew Provenza

Glenn Research Center, Cleveland, Ohio

Ralph Jansen and Ben Ebihara

University of Toledo, Toledo, Ohio

Alan Palazzolo

Texas A&M University, College Station, Texas

DISTRIBUTION STATEMENT A

Approved for Public Release

Distribution Unlimited

20031103 151

The NASA STI Program Office . . . in Profile

Since its founding, NASA has been dedicated to the advancement of aeronautics and space science. The NASA Scientific and Technical Information (STI) Program Office plays a key part in helping NASA maintain this important role.

The NASA STI Program Office is operated by Langley Research Center, the Lead Center for NASA's scientific and technical information. The NASA STI Program Office provides access to the NASA STI Database, the largest collection of aeronautical and space science STI in the world. The Program Office is also NASA's institutional mechanism for disseminating the results of its research and development activities. These results are published by NASA in the NASA STI Report Series, which includes the following report types:

- **TECHNICAL PUBLICATION.** Reports of completed research or a major significant phase of research that present the results of NASA programs and include extensive data or theoretical analysis. Includes compilations of significant scientific and technical data and information deemed to be of continuing reference value. NASA's counterpart of peer-reviewed formal professional papers but has less stringent limitations on manuscript length and extent of graphic presentations.
- **TECHNICAL MEMORANDUM.** Scientific and technical findings that are preliminary or of specialized interest, e.g., quick release reports, working papers, and bibliographies that contain minimal annotation. Does not contain extensive analysis.
- **CONTRACTOR REPORT.** Scientific and technical findings by NASA-sponsored contractors and grantees.

- **CONFERENCE PUBLICATION.** Collected papers from scientific and technical conferences, symposia, seminars, or other meetings sponsored or cosponsored by NASA.
- **SPECIAL PUBLICATION.** Scientific, technical, or historical information from NASA programs, projects, and missions, often concerned with subjects having substantial public interest.
- **TECHNICAL TRANSLATION.** English-language translations of foreign scientific and technical material pertinent to NASA's mission.

Specialized services that complement the STI Program Office's diverse offerings include creating custom thesauri, building customized databases, organizing and publishing research results . . . even providing videos.

For more information about the NASA STI Program Office, see the following:

- Access the NASA STI Program Home Page at <http://www.sti.nasa.gov>
- E-mail your question via the Internet to help@sti.nasa.gov
- Fax your question to the NASA Access Help Desk at 301-621-0134
- Telephone the NASA Access Help Desk at 301-621-0390
- Write to:
NASA Access Help Desk
NASA Center for AeroSpace Information
7121 Standard Drive
Hanover, MD 21076



Room Temperature Characterization of a Magnetic Bearing for Turbomachinery

Gerald Montague

U.S. Army Research Laboratory, Glenn Research Center, Cleveland, Ohio

Mark Jansen

Sest, Inc., Brook Park, Ohio

Andrew Provenza

Glenn Research Center, Cleveland, Ohio

Ralph Jansen and Ben Ebihara

University of Toledo, Toledo, Ohio

Alan Palazzolo

Texas A&M University, College Station, Texas

National Aeronautics and
Space Administration

Glenn Research Center

Acknowledgments

This research was funded by NASA Glenn Research Center's Smart Efficient Components program (SEC), which is managed by Bob Corrigan. The authors would like to thank Peter Kascak (University of Toledo) for his assistance in the power measurement, John Poles (NASA Glenn) for his significant electrical contributions, and Tim Czaruk (QSS Group, Inc.) for test support. The authors would also like to recognize Gerald Brown and Albert Kascak (NASA Glenn) for their expert guidance and review. Finally, we praise Texas A&M students Randy Tucker, Jason Preuss, and Andrew Hunt who designed and constructed the high temperature coils used in this bearing.

The Aerospace Propulsion and Power Program at
NASA Glenn Research Center sponsored this work.

Available from

NASA Center for Aerospace Information
7121 Standard Drive
Hanover, MD 21076

National Technical Information Service
5285 Port Royal Road
Springfield, VA 22100

Available electronically at <http://gltrs.grc.nasa.gov>

Room Temperature Characterization of a Magnetic Bearing for Turbomachinery

Gerald Montague
U.S. Army Research Laboratory
National Aeronautics and Space Administration
Glenn Research Center
Cleveland, Ohio 44135

Mark Jansen
Sest, Inc.
Brook Park, Ohio 44142

Andrew Provenza
National Aeronautics and Space Administration
Glenn Research Center
Cleveland, Ohio 44135

Ralph Jansen and Ben Ebihara
University of Toledo
Toledo, Ohio 43606

Alan Palazzolo
Texas A&M University
College Station, Texas 77843

ABSTRACT

Open loop, experimental force and power measurements of a three-axis, radial, heteropolar magnetic bearing at room temperature for rotor speeds up to 20,000 RPM are presented in this paper. The bearing, NASA Glenn Research Center's and Texas A&M's 3rd generation high temperature magnetic bearing, was designed to operate in a 1000 °F (540 °C) environment and was primarily optimized for maximum load capacity. The experimentally measured force produced by one C-core of this bearing was 630 lb. (2.8 kN) at 16 A, while a load of 650 lbs (2.89 kN) was predicted at 16 A using 1D circuit analysis. The maximum predicted radial load for one of the three axes is 1,440 lbs (6.41 kN) at room temperature. The maximum measured load of an axis was 1050 lbs. (4.73 kN). Results of test under rotating conditions showed that rotor speed has a negligible effect on the bearing's load capacity. A single C-core required approximately 70 W of power to generate 300 lb (1.34 kN) of magnetic force. The room

temperature data presented was measured after three thermal cycles up to 1000 °F (540 °C), totaling six hours at elevated temperatures.

INTRODUCTION

The gas turbine industry has a continued interest in improving engine performance and reducing net operating and maintenance costs. These goals are being realized because of advancements in aeroelasticity, materials, and computational tools such as CFD and engine simulations. These advancements aid in increasing engine thrust-to-weight ratios, specific fuel consumption, pressure ratios, and overall reliability through engine operation at higher rotational speeds and higher temperatures with greater efficiency.

Rolling element bearings and squeeze film dampers are currently used to support gas turbine engine rotors. The bearings presently in operation are limited in temperature (<500 °F, 270 °C) and speed (DN <2 million), and require

both cooling air and a lubrication system. Rolling element bearings in gas turbines are being pushed to their limits and new technologies must be found in order to take full advantage of other engine advancements.

Magnetic bearings are well suited to operate at elevated temperature and higher rotational speeds and are a promising solution to these problems. Magnetic bearing technology is being developed worldwide and is considered an enabling technology for new engine designs. Turbine and compressor spools can be designed with higher operating temperatures and significantly larger, stiffer, highly damped rotors, which spin at higher rotational speeds. Magnetic bearings will allow compressor, turbine, combustor, and nozzle advancements to reach their full performance potential.

Beams and Black performed some of the first research on magnetic suspension of rotating bodies [1] in 1937. An ultracentrifuge rotor, which was supported axially by compressed air, was replaced with a magnetic bearing. The vertical rotor position was so stable that no motion was detected with a 100X microscope and the reduction in power losses enabled operation at very high speeds.

Some of the first work on magnetic properties of soft materials at extreme temperatures was done at Westinghouse Electric in 1967 [2]. Information was gathered about eight selected materials for high temperature electric devices. More recently, Fingers from the U.S. Air Force Research Laboratory supported the more electric aircraft effort [3]. The major objective of this work was to replace mechanical systems with electrical devices in order to increase military aircraft reliability and maintainability while reducing ground support equipment.

The first high temperature magnetic bearing fabricated and tested at NASA Glenn was homopolar design with an electromagnetic bias coil. The second generation was a heteropolar design that minimized pole face area to enable maximum volume for high temperature coil design.

Data presented in this paper characterizes the 3rd generation high temperature, high load magnetic bearing developed at the NASA Glenn

Research Center at room temperature. Bearing force as a function of current and speeds to 20,000 RPM is presented. In addition, bearing power consumption measurements are made at several current levels.

TEST FACILITY

FACILITY DESCRIPTION

The high temperature magnetic bearing test facility is shown in Figure 1. The structural support can accommodate thrust and radial bearings up to 9.0 in (22.84 cm) diameter with a maximum axial loading of 5,000 lb (22.25 kN) and a maximum radial loading of 2,500 lb (11.13 kN). The test facility has already been used in several different configurations.

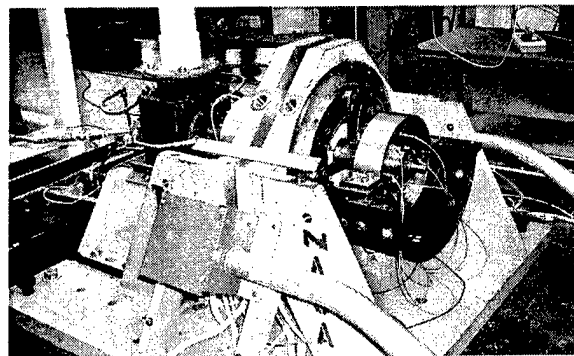


Figure 1 – High temperature magnetic bearing test facility at NASA Glenn Research Center.

The facility was previously used to measure linearized force coefficients (position and current stiffness and damping) of magnetic bearings versus speed, bias current, excitation frequency, and eccentricity. The second configuration was used to demonstrate stable rotor levitation and fault tolerance of a radial magnetic bearing at high temperature (1000 °F) up to 15,000 RPM [4, 5].

The present configuration can be seen in Figure 2. The magnetic bearing is located at the center of gravity of the 2.97 in (75 mm) diameter rotor. A 0.022 in (0.559 mm) radial air gap exists between the stator poles and the rotor. The rotor has interchangeable sleeves on each end that interface it with the support

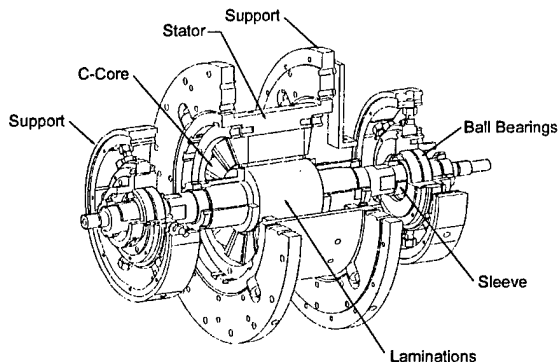


Figure 2 – Third generation high temperature magnetic bearing facility.

bearings, which currently are high-speed, grease packed, duplex ball bearings. For this configuration, the rotor was fitted with zero clearance sleeves so it is supported on the ball bearings at both ends. This was done so that static forces exerted by the magnetic bearing could be easily measured outside the hot section. The outboard sleeve can be replaced with a positive clearance sleeve so that the magnetic bearing can support the rotor. An air turbine drives the rotor.

The magnetic bearing stator is an isolated C-core, 12-pole, heteropolar design and is described in detail in Reference 5. The rotor diameter is 2.98 in. (75 mm) and the stator width is 3.4 in. (76.1 mm). Each C-core is wrapped with two coils and each coil has 52 turns of specially insulated wire.

Power to the magnetic bearing is provided through tri-state pulse width modulated (PWM) amplifiers that are passively filtered to remove high frequency amplifier noise that results from amplifier switching.

Heat is supplied to the bearing through three, 3 kW band heaters wrapped around the stator. Ground Fault Circuit Interrupts (GFCI) have been incorporated into the heating system for personnel safety.

SENSORS

The test rig is equipped with several types of sensors. High load, high bandwidth, piezoelectric load cells support the inboard and

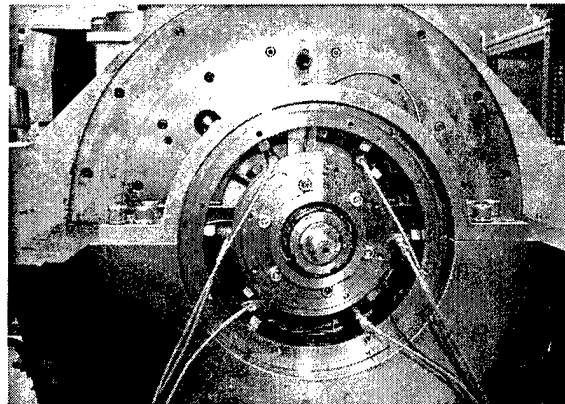


Figure 3 – Six load cells supporting the outboard duplex ball bearing.

outboard rolling element bearings (Figure 3). The load cells are resting on machined flats of the bearing housing. This load cell mounting design eliminates axial constraints of the ball bearing.

These load cells are capable of measuring loads up to 1,688 lb (7.5 kN) at 200 kHz and have a maximum operating temperature of 385 °F (196 °C). Two load cells are aligned along each of the three magnetic bearing axes on both support bearings for a total of 12 load cells. Each load cell was set with a preload of ~250 lb (1.1 kN).

High temperature eddy current displacement probes are used just outside the stator on both sides of the magnetic bearing to monitor rotor position. Each side has four probes (X+, X-, Y+, Y-) for a total of eight probes. The probes are capable of 30 μ in (1.18 μ m) accuracy and are temperature compensated for the 1000°F (538 °C) environment.

Temperatures are recorded at several locations within the test rig. Both sides of the stator have three thermocouples mounted to them. Each set of support ball bearings is also equipped with a thermocouple. A handheld infrared thermometer can also be used to gather additional thermal information about the shaft during rotation.

Other sensors include: an eddy current displacement probe used to measure rotor RPM and phase, current sensors to measure C-core

currents, and temperature and redundant RPM sensors in the air turbine.

DATA ACQUISITION

A LabVIEW-based data acquisition system is used in this facility. This system is capable of capturing data at rates up to 15,000 samples per second per channel. Data is recorded for the drive end and outboard load cells, support bearing temperatures, stator temperatures, X and Y axis displacement probes, once around probe, and bearing coil currents. Data is displayed in real time and can be saved directly into a spreadsheet format.

EXPERIMENTAL

For the tests reported in this paper, the shaft was mounted on zero clearance ball bearing supports so the load exerted by the magnetic bearing C-cores on the rotor could be measured.

ROTOR BOUNCE MODE

For a rigid rotor supported on two springs of stiffness K : $\omega_n = \sqrt{2K/m} = 24,143 \text{ RPM} = 2522 \text{ rad/s.}$, with $m = 17/386$, $K = 138,934 \text{ lb./in.}$ The mode was verified two different ways. First, a swept sine input was fed into the PWM amplifiers and a dynamic signal analyzer recorded the DC current to load cell output transfer function. Since the load cells and ball bearings provide little damping to the rotor, the first rotor bending critical was easily measured to be 407 Hz. Second, a rap test on the rotor produced a first resonance at 386 Hz. These results are in 95 percent agreement.

This resonance did not limit the maximum testing speed to 20,000 RPM. Rather, overheating of the unsealed, grease packed ball bearings at 20,000 RPM was the limiting factor.

ROTOR IMBALANCE FORCES

Rotor imbalance vs. rotational speed was determined so that this force could be accounted for in the DC load tests being performed at speed. Synchronous component amplitude and phase for all twelve-load cells were recorded with the magnetic bearing power

off up to 20,000 RPM. The maximum transmitted unbalance force measured by a load cell was 52 lb (23.5 kg) at 20,000 RPM. However, due to the load cell preload and the vector summation for load calculation, the rotor imbalance force cancels itself during data acquisition of the magnetic axis load measurements.

FORCE CHARACTERIZATION

THEORETICAL FORCE PREDICTIONS

For a general magnetic actuator, the force produced by magnetic flux in an air gap of area A_g is given by

$$F = \frac{1}{2} \alpha \mu_o A_g \left(\frac{NI}{2G} \right)^2 \quad (1)$$

In this equation, μ_o is the magnetic permeability of evacuated space, NI is the ampere-turns of the coil(s) driving the flux through the circuit, and $2G$ represents the total effective magnetic air gap. α is a force de-rating factor, which accounts for leakage, fringing, non-uniformity in flux density across the pole faces, and finite path permeability [6].

The actuator measurements documented in this paper are based on the performance of a complete c-core circuit. Consequently, the force produced by a single c-core is twice that obtained using equation 1, since there are two air gaps between it and the rotor.

Using $\mu_o = 4\pi \times 10^{-7} \text{ N/A}^2$, $N = 52 \times 2$ turns, $A_g = 2.0 \text{ in.}^2$ (12.9 cm^2), $G = 0.022 \text{ in.}$ (0.559 mm), $\alpha = 0.8$, and converting to Imperial units, yields:

$$F(I) = 2.53 \times I^2 \text{ lbf} \quad (2)$$

At 10 A, the force produced by C-core #1 is 253 lbf (1.1 kN). Since the total air gap area is 4 in.^2 (25.8 cm^2), the effective magnetic pressure produced by one C-core at 10 A is 63.3 psi (434 kPa).

Flux density vs. applied current data taken for similar heteropolar magnetic bearings made of Hyperco 50 laminations have shown that 2

Tesla is achievable in the air gap. Using the equation

$$B_{sat} = \frac{\mu_o NI_{sat}}{2G} \quad (3)$$

and solving for I_{sat} with $B_{sat} = 2$ T yields 16.9 A. The maximum force capacity of a C-core then from equation (2) becomes 720 lbf (3.2 kN), which corresponds to an effective magnetic pressure of 180 psi (1,241 kPa).

The saturation flux density of 2 Teslas used here for predicting the saturation current is selected somewhat arbitrarily. Typically B_{sat} is selected as the point on the static B-H material data curve where linearity is lost and the curve heels over towards a final slope of μ_o . 2 Teslas may not be that point for this material. One way to determine B_{sat} is to insert a hall-effect probe in the gap of the c-core and measure flux density as a function of c-core current. This test will be performed for a future paper.

For this 12 pole, isolated C-core bearing oriented as shown in Figure 4, the maximum radial force can be produced only in the X direction. A maximum positive force will be produced when C-cores #2,3,4 are driven with 16.9 A, and C-cores #1,5,6 are not used at all. Notice that all six C-cores can contribute to the production of an X force, but only four can contribute to a Y force. In the X-direction, the maximum radial force that can be produced by this bearing is 1,440 lbf (6.4kN).

Although this 3rd generation high temperature magnetic bearing was optimized for load capacity, the stator poles do not completely cover the rotor. To determine the effective maximum radial pressure, the maximum force must be divided by the net hemispheric surface area of the rotor. The outer diameter of the rotor is 2.97 in. (75.4 mm) and the stator poles are 3.4 in. (86.4 mm) long, making the net surface area 16 in.² (103 cm²). Thus, the net effective maximum pressure produced by this bearing is 90 psi (620 kPa).

MAXIMUM FORCE CAPABILITY OF A SINGLE CORE

The first test run was to determine the maximum load capacity of a single core and the current level where saturation is reached. This was done by attaching the coil directly to a high power DC supply (100V, 40A) and measuring load as a function of current. Load remains constant as current increases due to flux saturation in the lamination material. The #1 C-core was tested and the results are shown in Figure 5.

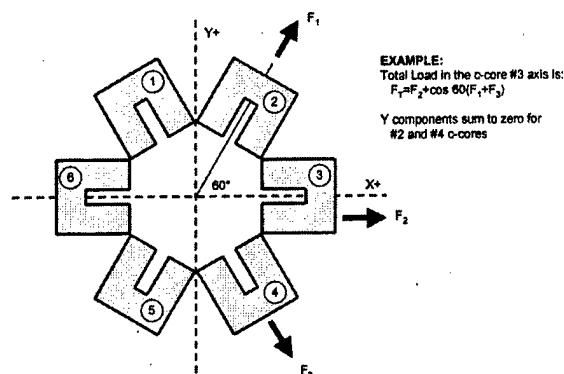


Figure 4 – Total load on each magnetic axis is a sum of the force from three C-cores.

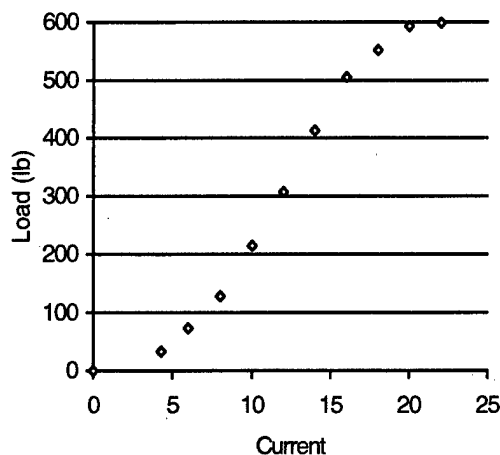


Figure 5 – Maximum load and saturation level for C-core #1 using the DC power supply.

DC POWER SUPPLY VERSUS PULSE WIDTH MODULATION POWER SUPPLY

Power to the magnetic bearing is normally supplied by a pulse width modulation (PWM) power supply. This type of power supply is more efficient than a direct DC supply. For this facility, the practical output limit of the PWM supplies is 15 Amps. Since the saturation level of the bearing occurs at around 21 Amps, the DC supply was used. In order to assure that accurate data could be attained with the PWM supplies, a comparison was done between the PWM loads and the loads attained with two different DC supplies. There is almost exact correlation between all three. The results are shown in Figure 6.

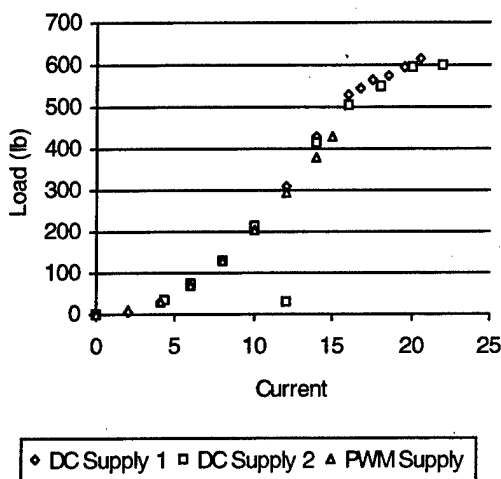


Figure 6 – Comparison of loads obtained with PWM supplies and two DC power supplies (C-core #1).

INDIVIDUAL C-CORE LOAD CAPACITY

The next series of tests run were to determine the load capacity of a single C-core as a function of current. Connecting a constant current supply to the power amplifiers and measuring the load at steady-state conditions achieved this.

Each C-core was measured for load capacity at 0 RPM and compared with one another. These results are shown in Figure 7 and summarized in Table 1. Discrepancy between the C-cores will be discussed later in this paper. Once each C-core load capacity was determined, the tests

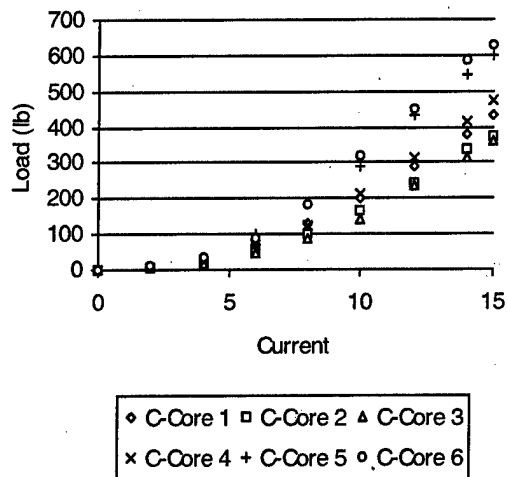


Figure 7 – Load as a function of current for individual C-cores.

Table 1 – Summary of single C-core load (lb) capacity up to 15 amps at zero RPM.

C-Core	6 Amp Load	10 Amp Load	15 Amp Load
1	71	203	431
2	56	167	374
3	49	140	363
4	72	212	473
5	101	291	597
6	90	320	630

to determine the load capacity along a magnetic axis and at rotor speeds to 20,000 RPM were performed.

LOAD CAPACITY OF AN AXIS

The second series of tests run were to determine the load capacity on an axis. The maximum load on an axis is a function of three adjacent C-cores. The two C-cores on either side of the main axis have a contribution to the total load in that axis (Figure 4). Static tests were performed to check if all the C-cores had similar load capacity.

The total force along each magnetic axis is the sum of the forces from three C-cores (Figure 4). For example, in the #3 C-core direction, the total force is the sum of the #3 C-core, and the x-components from the #2 and #4 C-core. The y-components of force from the #2 and #4 coil

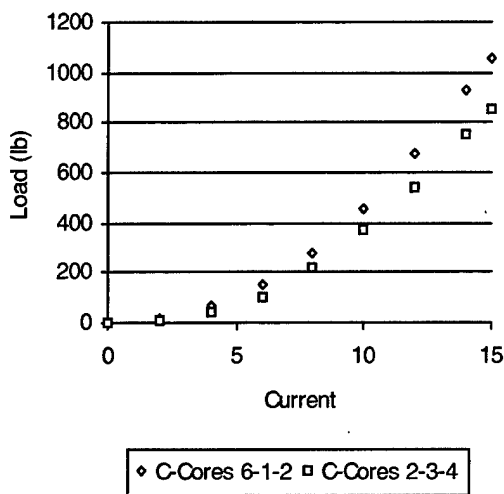


Figure 8 – Load as a function of current for two magnetic axes at zero RPM.

Table 2 – Resultant load (lb) along two magnetic axis capacity up to 15 amps at zero RPM.

Magnetic Axis	6 Amp Load	10 Amp Load	15 Amp Load
6-1-2	151	460	1056
2-3-4	128	369	853

are equal and opposite and therefore cancel each other.

The results of load vs. current at 0 RPM for each magnetic axis are shown in Figure 8 and summarized in Table 2.

To confirm the load of the magnetic axis was applied in the same direction as the center C-core of that axis, the angle at which the load was applied was also monitored. The angles matched the theoretical value (i.e. 120° for the #6-1-2 axis) within a few degrees.

The discrepancy in the load capacity of the C-cores and also of the magnetic axis could be related to a non-uniform air gap between the rotor and stator. A dial indicator was used to measure 0.0005-0.001" rotor lamination run-out. Plastic feeler gages were used to verify the non-uniform air gap. A minimum gap of 0.015" was measured. The eight displacement sensors monitored position during all the tests to ensure the rotor did not bow or change position relative to the support stand. However, the stator was

Table 3 – Coil load vs. average load at zero RPM.

Amp	Ave. Load	#1	#2	#3	#4	#5	#6
2	7	1	-1	-2	-1	2	3
4	28	2	-3	-8	-3	5	7
6	73	-2	-17	-24	-1	28	17
8	136	-7	-33	-47	-9	48	49
10	222	-19	-55	-82	-10	69	98
12	329	-36	-83	-91	-16	103	122
14	430	-52	-91	-114	-12	114	156
15	478	-47	-104	-115	-5	119	152

not monitored and its position may have changed slightly due to slipping, thus changing the air gap between the coils.

A reduction in air gap would result in an increase in the measured force. If this were the case, the air gap between the 180° opposite C-core should increase and correspondingly the force measured would be lower. Table 3 shows the average value of all six single core measurements and their deviation from the average. The trend of opposite C-cores have approximately equal and opposite deviations from the average is observed. (1 vs. 4, 2 vs. 5, 3 vs. 6). This trend is also observed from Figure 7.

Another explanation for the force differences could be a slight difference in PWM amplifier gain. However, all six PWM amplifiers were tuned identically. Also, the load cell signal conditioners were set-up identically and statically tested in the rig with a mechanical force applicator.

During build-up of the facility, the air gap was maintained during rotor alignment by inserting plastic shims between the rotor and stator. When the rig was fully assembled, accurate measurement of the air gap was nearly impossible. In the future, a high temperature displacement sensor could be used to monitor the stator position.

SPEED DEPENDENCE OF LOAD CAPACITY

Data was also taken for C-core #1 at speeds up to 20,000 RPM and various currents. This data is shown graphically in Figure 9 and summarized in Table 4.

Figure 9 shows no force reduction due to the rotating laminated rotor at room temperature with a uniform air gap using open loop control.

The authors recognize that there are frictional forces generated within the rolling element bearings that are not accounted for in these results. However, the bearings provide a good load path from the rotating shaft. The option of measuring forces at the stator (Figure 10) has been tried prior to this publication. The problem with this method was that the load cells have to be in line with the stator mechanical support and an actuator system is required. This permits stator deflection and position slips during dynamic tests.

Since there is little dependence of force on rotor speed, it can be inferred that rotor surface speed does not cause significant eddy current or hysteretic effects. Both may still have significant effects on actuator bandwidth.

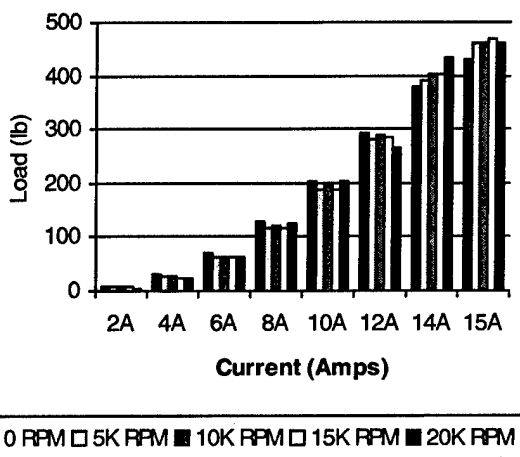


Figure 9 – C-core #1 load as a function of rotor speed for bearing currents up to 15 amps.

Table 4 – Summary of load (lb) for C-core #1 up to 20,000 RPM.

Shaft RPM	6 Amp Load	10 Amp Load	15 Amp Load
0	71	188	459
5,000	61	197	459
10,000	64	189	468
15,000	63	204	462
20,000	63	201	455

POWER CHARACTERIZATION

POWER CONSUMPTION OF SINGLE CORE

The power required by the bearing cores as a function of magnetic force, current was also determined. At room temperature, the average resistance (R) for a C-core (2 coils) is 0.48 Ohms and inductance (L) is 18mH. The real power used by the C-core is a function of the output voltage of the pulse width modulation amplifier (22 kHz switching frequency) and the instantaneous current. Figure 11 shows the typical power system for one C-core.

The high switching frequency of the PWM amplifier made it difficult to measure the power required for this magnetic bearing. Normal 60 cycle RMS power measurements cannot be applied.

Due to the high cycle frequency signal, a high-speed scope (1 million samples/sec.) was used to record the instantaneous voltage across the coil and the instantaneous current through the coil. The isolated, high impedance scope collected 41,000 samples (41 ms) for the single C-core tests. Average power for that time was

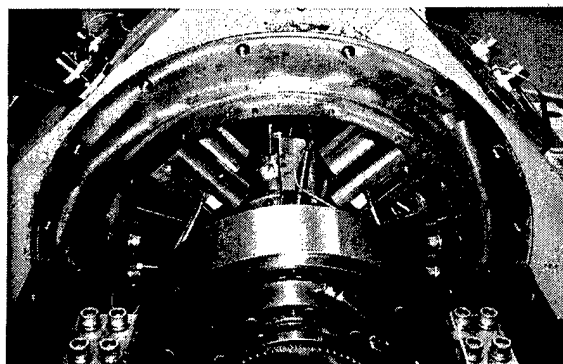


Figure 10 – Load measurements at the stator using piezoelectric actuators.

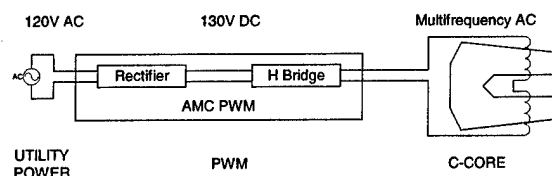


Figure 11 – Power system for one C-Core.

calculated using a zero power factor. When data was collected for one magnetic axis (3 C-cores), the number of samples was reduced to 10,000 samples (10 ms) in order to have a manageable size data file.

POWER MEASUREMENTS

Average power was calculated for individual C-cores and the #6-1-2 magnetic axis at zero RPM. The power for the magnetic axis is the sum of the power from the three C-cores in that axis. All the power calculations are shown in Figure 12 and summarized in Table 5.

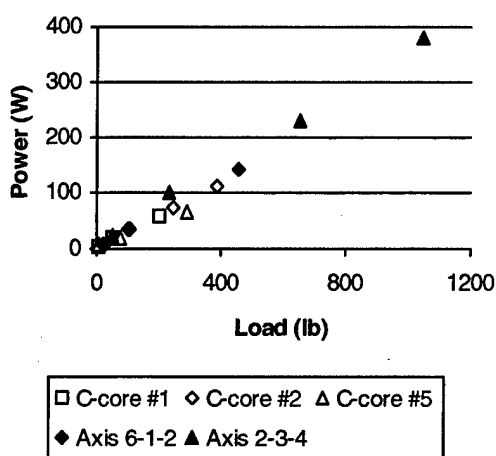


Figure 12 – Power consumption using PWM supplies at zero RPM.

Table 5 – Summary of power (W) using PWM power supplies and load (lb) as a function of input current at 0 RPM.

#	2 Amp	4 Amp	5 Amp	8 Amp	10 Amp	15 Amp
#1	4 W 7 lb	N/A	19 W 53 lb	N/A	59 W 203lb	N/A
#2	N/A	8 W 26 lb	N/A	33 W 102lb	N/A	113W 385lb
#5	9 W 9 lb	N/A	18 W 77 lb	N/A	66 W 291lb	N/A
#2-3-4	N/A	24 W 48 lb	N/A	100W 233lb	N/A	380W 1048lb
#6-1-2	8 W 18 lb	N/A	36 W 105lb	N/A	142W 460lb	N/A

CONCLUDING REMARKS

Although the shaft is not doing any work and the rotor is not levitated, magnetic force and electrical power for a high load, high speed, room temperature radial magnetic bearings for

turbomachinery were measured. These baseline measurements are important in order to provide industry performance characteristics for actual hardware and in assessing issues such as non-uniform air gaps. This high temperature magnetic bearing can apply over 400 lbs./axis (1.78 kN/axis) using less power than three household light bulbs. Loads up to 1050 lb (4.7 kN) per magnetic axis were achieved. No measurable force reduction was observed due to rotation up to 20,000 RPM. The discrepancy between the theoretically predicted force and the measured is most likely the result of a non-uniform air gap (un-centered rotor), and or a degradation of lamination magnetic properties due to thermal cycling. Further work will address these issues and will include force and power measurements at high temperature. High temperature, high-speed levitation tests will also be conducted without the use of rolling element bearings. Characterization tests similar to those presented in this paper are underway at 1000 °F (540 °C) and will be presented in a later paper.

REFERENCES

- 1.) Beams, J.W., Black, S.A., "Electrically-Driven, Magnetically-Supported, Vacuum-Type Ultracentrifuge," Vol. 10, pp.59–63, Feb. 1939.
- 2.) Kueser, P.E., Pavlovic, D.M., Lane, D.H., Clark, J.J., and Spewock, M. "Properties of Magnetic Materials for use in High-Temperature Space Power Systems," NASA SP-3043, 1967.
- 3.) Fingers, R.T., "Creep Behavior of Thin Laminates of Iron Cobalt Alloys for Use In Switch Reluctance Motors and Generators," Air Force Research Laboratory AFRL-PR-WR-TR-199-2053, 1999.
- 4.) Minihan, T., Palazzolo, A., Montague, G.T., Kascak, A.F., Provenza, A., "Fail Safe, High Temperature Magnetic Bearings," IGTI ASME Turbo Expo, Amsterdam June 3–6, 2002.
- 5.) Choi, B., and Montague, G.T., "Fail-safe Operation of a High Temperature Magnetic Bearing for Turbomachinery," 6th International Symposium on Magnetic Suspension Technology.
- 6.) Jansen, R.H., Ebihara, B.E., Montague, G.T., Provenza, A.J., Jansen, M.J., Palazzolo, A., Tucker, R., Preuss, J., Hunt, A., "Design and Construction of a High Temperature, High Load Radial Magnetic Bearing for Turbomachinery," NASA TM to be published, 2002.
- 7.) *Introduction to Magnetic Bearings*, University of Virginia Short Course, presented at the Third International Symposium on Magnetic Bearings, Alexandria, Virginia, 1993.

REPORT DOCUMENTATION PAGE			Form Approved OMB No. 0704-0188	
Public reporting burden for this collection of information is estimated to average 1 hour per response, including the time for reviewing instructions, searching existing data sources, gathering and maintaining the data needed, and completing and reviewing the collection of information. Send comments regarding this burden estimate or any other aspect of this collection of information, including suggestions for reducing this burden, to Washington Headquarters Services, Directorate for Information Operations and Reports, 1215 Jefferson Davis Highway, Suite 1204, Arlington, VA 22202-4302, and to the Office of Management and Budget, Paperwork Reduction Project (0704-0188), Washington, DC 20503.				
1. AGENCY USE ONLY (Leave blank)	2. REPORT DATE October 2002	3. REPORT TYPE AND DATES COVERED Technical Memorandum		
4. TITLE AND SUBTITLE Room Temperature Characterization of a Magnetic Bearing for Turbomachinery		5. FUNDING NUMBERS WU-708-28-13-00 1L161102AF20		
6. AUTHOR(S) Gerald Montague, Mark Jansen, Andrew Provenza, Ralph Jansen, Ben Ebihara, and Alan Palazzolo				
7. PERFORMING ORGANIZATION NAME(S) AND ADDRESS(ES) National Aeronautics and Space Administration John H. Glenn Research Center at Lewis Field Cleveland, Ohio 44135-3191		8. PERFORMING ORGANIZATION REPORT NUMBER E-13594		
9. SPONSORING/MONITORING AGENCY NAME(S) AND ADDRESS(ES) National Aeronautics and Space Administration Washington, DC 20546-0001 and U.S. Army Research Laboratory Adelphi, Maryland 20783-1145		10. SPONSORING/MONITORING AGENCY REPORT NUMBER NASA TM-2002-211904 ARL-TR-2858		
11. SUPPLEMENTARY NOTES Gerald Montague, U.S. Army Research Laboratory, NASA Glenn Research Center; Mark Jansen, Sest, Inc., 18000 Jefferson Park Road, Suite 104, Middleburg Heights, Ohio 44130; Andrew Provenza, NASA Glenn Research Center; Ralph Jansen and Ben Ebihara, University of Toledo, 2801 W. Bancroft Street, Toledo, Ohio 43606-3328; and Alan Palazzolo, Texas A&M University, College Station, Texas 77843. Responsible person, Gerald Montague, organization code 0300, 216-433-6252.				
12a. DISTRIBUTION/AVAILABILITY STATEMENT Unclassified - Unlimited Subject Categories: 07, 09 and 15 Available electronically at http://gltrs.grc.nasa.gov This publication is available from the NASA Center for AeroSpace Information, 301-621-0390.			12b. DISTRIBUTION CODE	
13. ABSTRACT (Maximum 200 words) Open loop, experimental force and power measurements of a three-axis, radial, heteropolar magnetic bearing at room temperature for rotor speeds up to 20,000 RPM are presented in this paper. The bearing, NASA Glenn Research Center's and Texas A&M's third generation high temperature magnetic bearing, was designed to operate in a 1000 °F (540 °C) environment and was primarily optimized for maximum load capacity. The experimentally measured force produced by one C-core of this bearing was 630 lb. (2.8 kN) at 16 A, while a load of 650 lbs (2.89 kN) was predicted at 16 A using 1D circuit analysis. The maximum predicted radial load for one of the three axes is 1,440 lbs (6.41 kN) at room temperature. The maximum measured load of an axis was 1050 lbs. (4.73 kN). Results of test under rotating conditions showed that rotor speed has a negligible effect on the bearing's load capacity. A single C-core required approximately 70 W of power to generate 300 lb (1.34 kN) of magnetic force. The room temperature data presented was measured after three thermal cycles up to 1000 °F (540 °C), totaling six hours at elevated temperatures.				
14. SUBJECT TERMS Turbomachinery; Magnetic bearing; C-core; Power factor			15. NUMBER OF PAGES 15	
			16. PRICE CODE	
17. SECURITY CLASSIFICATION OF REPORT Unclassified	18. SECURITY CLASSIFICATION OF THIS PAGE Unclassified	19. SECURITY CLASSIFICATION OF ABSTRACT Unclassified	20. LIMITATION OF ABSTRACT	